

# On the origin of differential phase contrast at a locally charged and globally charge-compensated domain boundary in a polar-ordered material

## Supplementary Material

Ian MacLaren<sup>1</sup>, LiQiu Wang<sup>1</sup>, Damien McGrouther<sup>1</sup>, Alan J. Craven<sup>1</sup>, Stephen McVitie<sup>1</sup>, Roland Schierholz<sup>2</sup>, Andras Kovács<sup>3</sup>, Juri Barthel<sup>3,4</sup>, Rafal E. Dunin-Borkowski<sup>3</sup>

<sup>1</sup> SUPA School of Physics and Astronomy, University of Glasgow, Glasgow G12 8QQ, UK

<sup>2</sup> Institute of Energy and Climate Research: Fundamental Electrochemistry (IEK-9), Forschungszentrum Jülich, 52425 Jülich, Germany.

<sup>3</sup> Ernst-Ruska-Centre for Microscopy and Spectroscopy with Electrons (ER-C) and Peter Grünberg Institute (PGI), Forschungszentrum Jülich, 52425 Jülich, Germany.

<sup>4</sup> Central Facility for Electron Microscopy, RWTH Aachen University, 52074 Aachen, Germany.

### Simulation of diffraction patterns from perfect crystal

Figure S1 shows simulations of [100] diffraction patterns for pseudotetragonal cells of BiFeO<sub>3</sub> with different polarisation values, which have been calculated for a wide range of thicknesses. These show that whilst there is noticeable left-right asymmetry between opposed diffraction spots, polarisation alone does not change the symmetry of the bright field disc, as would be expected.

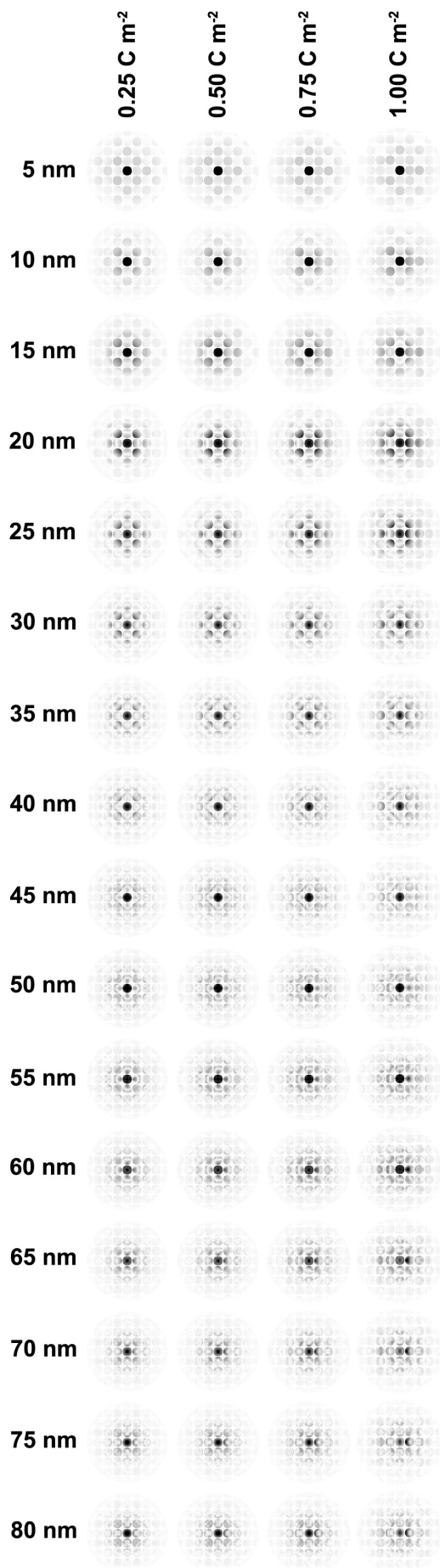


**Figure S1:** Simulations of [100] convergent beam electron diffraction patterns for a pseudotetragonal unit cell of BiFeO<sub>3</sub> with four different values of polarisation and a range of specimen thicknesses from 5 to 80 nm. The polarisation direction, [001], points towards the right. In every case, there is a contrast asymmetry between the 001 and 00 $\bar{1}$  diffraction spots. There is never any asymmetry in the bright-field spot. The diffraction patterns were calculated using MBFIT software [1], with 101 beams in the zeroth order Laue zone from 000 to {044}.

### The charge, field and polarisation distribution around the APB

Figure S2 shows the model for the APB. The boundary itself contains significant negative charge in the form of excess oxygen atoms, and this was estimated previously at  $-0.68 \text{ Cm}^{-2}$  by atom counting in the 3D atomic model [2]. This would, in the absence of any other surrounding material result in a perpendicular  $\mathbf{E}$ -field. Since this is in material, we have to consider this in terms of a  $\mathbf{D}$ -field including contributions from both  $\mathbf{E}$  and  $\mathbf{P}$ . As a result of the excess positive charge in the matrix, the  $\mathbf{D}$ -field is reduced as one goes away from the boundary according to Gauss' law:

$$\nabla \cdot \mathbf{D} = \varepsilon_0 \nabla \cdot \mathbf{E} + \nabla \cdot \mathbf{P} = \rho_c, \quad (1)$$

According to measurements of the polarisation from the atomic movements quantified using HRSTEM [2],  $\mathbf{P}$  falls to zero in about 7 unit cells of perovskite. The obvious boundary conditions for a solution of equation [1] are that  $\mathbf{E}$  and  $\mathbf{D}$  are zero far from the boundary. Thus,  $\mathbf{D} = 0$  after about 7 cells for our case and consequently  $\nabla \cdot \mathbf{D} = 0$  after about 7 cells. The boundary conditions therefore force a situation where  $\mathbf{E}$  and  $\nabla \cdot \mathbf{E}$  are also zero after 7 unit cells. This steady drop in  $\nabla \cdot \mathbf{D}$  with distance must correspond to a  $\rho_c$  corresponding to positive charge distributed in this region. This could be provided in the material by the excess charge from the  $\text{Ti}^{4+}$  doping at  $+e$  per Ti atom if the Ti concentration in this region is about 14% of B-sites. This requires that all the Ti atoms are effectively fully ionised – 3 electrons per atom would be devoted to bonding in the  $\text{TiO}_6^{3-}$  octahedra. The consequence of this is that a free electron is donated to the material. The obvious destination for these donated electrons would be the excess oxygen atoms in the boundary to ensure that all are fully ionised to  $\text{O}^{2-}$ . This would therefore set up a stable structure where the boundary is negatively charged and the surrounding matrix is positively charged – which could explain our polarisation profile in accordance with Gauss' law.

Please note, that there is no evidence for any free charges (e.g. free electrons) in this material at room temperature. These boundaries interlock in three dimensions in this material and if there were free electrons associated with these boundaries, they would contribute to boundary conductivity that would be significant and measurable. The conductivity of this material is below  $1 \mu\text{S cm}^{-1}$  and there is no separate boundary contribution[3] thus there are no free electrons at room temperature, supporting the fact that any free electrons from ionisation of Ti dopants have been transferred to other atoms – most likely O atoms, such as in the boundaries.

The required doping level for this effect is slightly above the target doping level of 10%, but not unreasonable. Such a structure could well have arisen during sintering as a charge-compensation mechanism to deal with the excess positive charge otherwise present in the matrix due to the high Ti doping level. The additional enrichment close to the boundary could have easily formed via electrostatic effects during sintering in order to minimise the internal electric fields. It should be noted that the boundary conditions therefore require that the total positive charge outside the boundary is equal to that in the negatively charged boundary, i.e. that there is global charge neutrality.

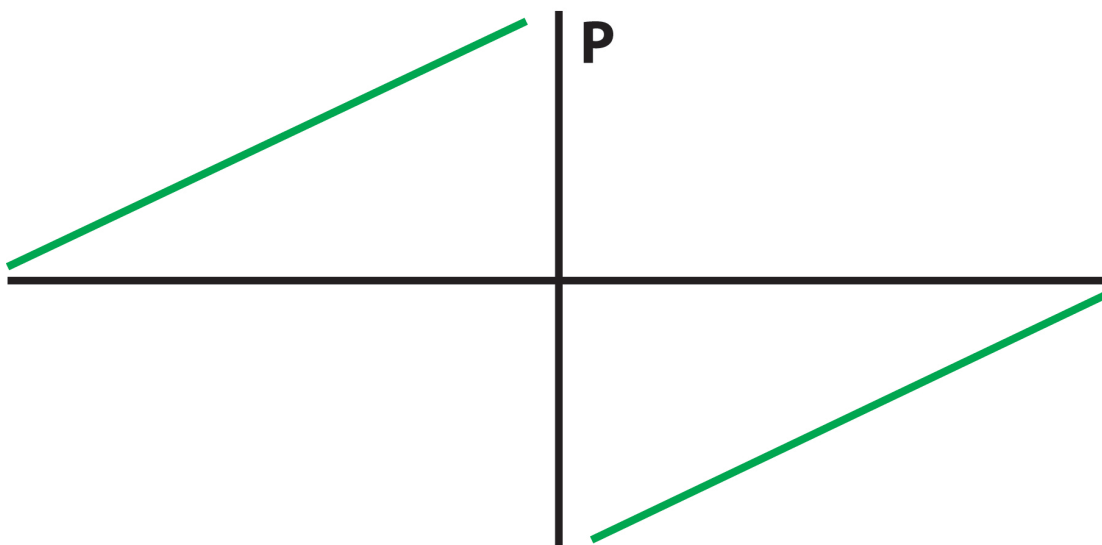
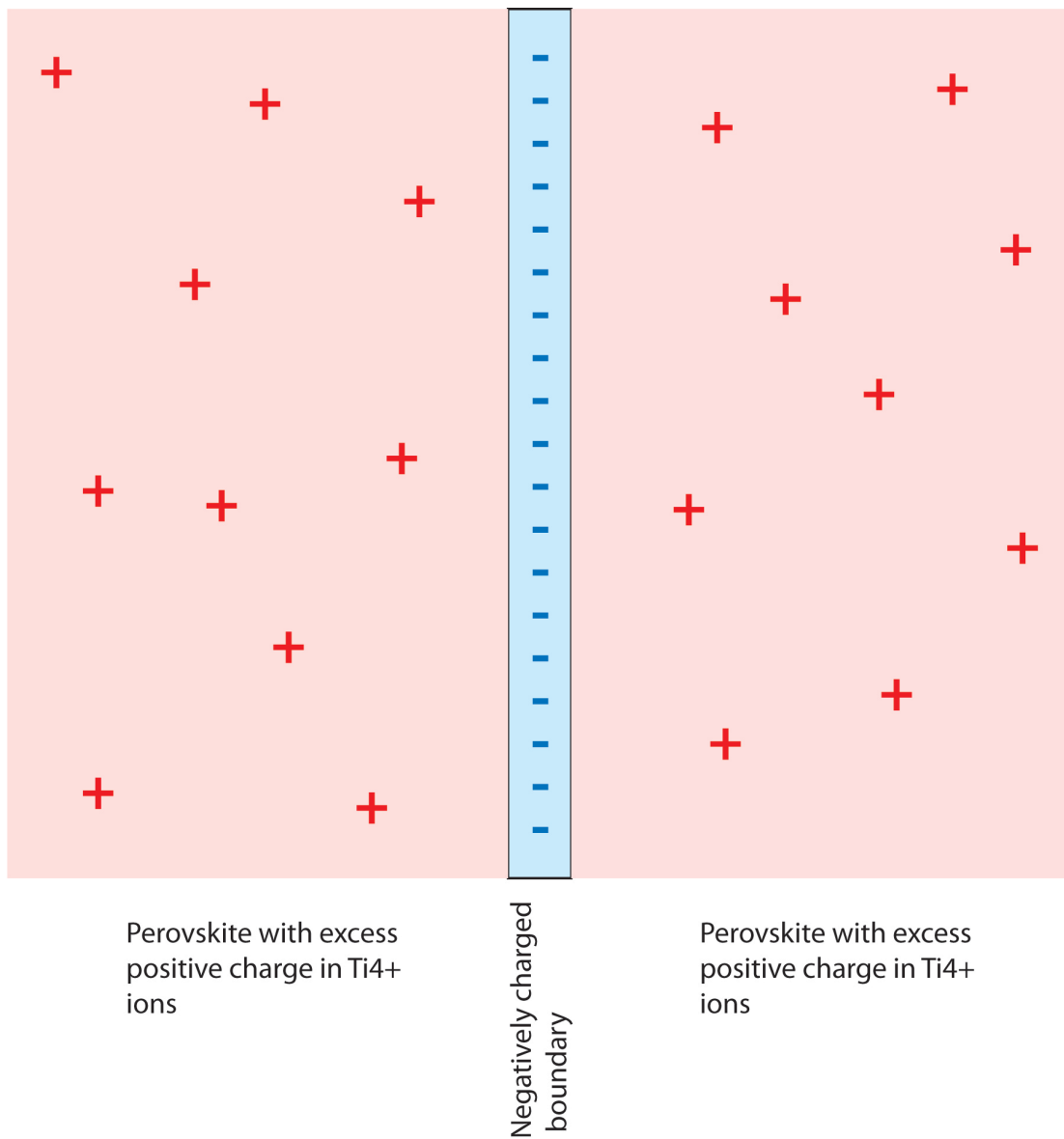


Figure S2: Schematic model of the negatively charged antiphase boundary and its surroundings used in the experiments, based on the observations published previously [2].

There are basically three possible solutions to equation (1) for these boundary conditions:

1. There is no polarisation and just  $\mathbf{E}$  in this region – this is like pure electrostatics in vacuum with no dielectric response of the material to  $\mathbf{D}$  and fixed charges.  $\mathbf{P}$  is zero everywhere. This is obviously not the case in our material, since  $\mathbf{P}$  has already been shown to follow the behaviour sketched in the lower part of Figure S2 (see also reference [2]).
2. There is some mixture of  $\mathbf{E}$  and  $\mathbf{P}$  in the 7 cells around the boundary with both tending to zero at its edge. This would, for instance, occur for the typical linear dielectric response of many insulators. This is called partial dielectric screening. We know from our experiments, that the  $\mathbf{E}$  field is negligible in this region, as we are seeing no detectable disc shifts in scanned diffraction. Thus, we must conclude that this is not the solution in our case.
3. The last possible solution is that  $\mathbf{P}$  is the only contributor to  $\mathbf{D}$  and that  $\mathbf{E}$  is zero everywhere, which is to say that the  $\mathbf{D}$  field is perfectly screened by polarisation and falls away to zero because of some excess fixed positive charge from Ti excess given by  $\rho_c$  in this layer of about 7 cells thick.

Please note, beyond about 7 units cells from the APBs, a different charge compensation mechanism comes into play to deal with the excess positive charge from ionisation of the excess titanium doping. This results in the formation of novel Nd-core nanorod structures via the formation of Nd vacancies [4, 5].

### Supercells and scanning diffraction simulations

The scanning diffraction simulations were performed using the supercells shown in Figure S3. Figure S3a) shows the supercell used in the calculation of Figure 4 in the paper.

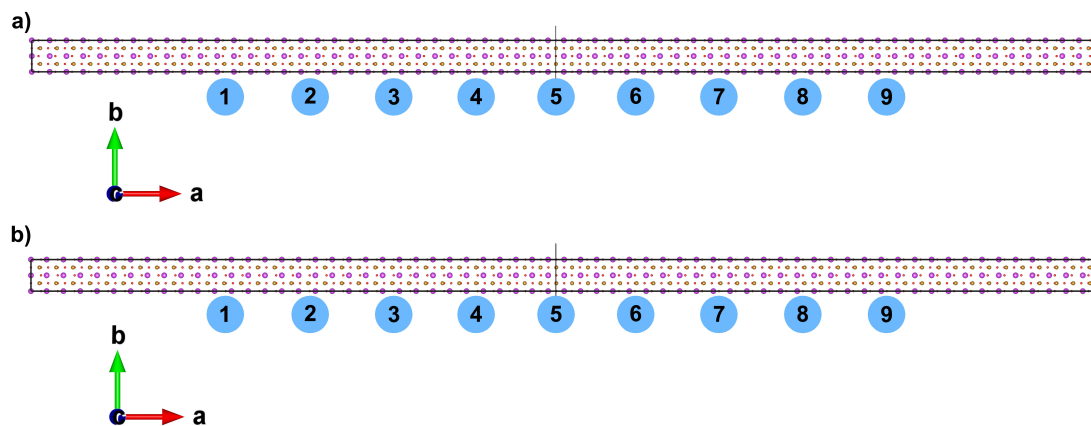


Figure S3: Supercells of a) Head-to-head; and b) Tail-to-tail arrangements of polarised  $\text{BiFeO}_3$  with a polarisation of  $1 \text{ C m}^{-2}$  away from the interface ( $100 \mu\text{C cm}^{-2}$ ). Approximate probe positions for the CBED simulations are shown.

In the case of the tail-to-tail simulation, the supercell of Figure S3b) gave the diffraction patterns shown in Figure S4. These show similar features to those shown in Figure 4 in the paper for the head-to-head case. Again, far from the boundary, there is some asymmetry in the diffracted spots, but no asymmetry in the bright field disc. As would

be expected, the direction of the asymmetry in the diffracted spots is opposite to that shown in Figure 4, since the directions of polarisation are reversed. In addition, immediately to the left or right of the boundary, there is a significant asymmetry with the bright field, which is exactly the same as seen in Figure 4, purely due to the boundary itself.

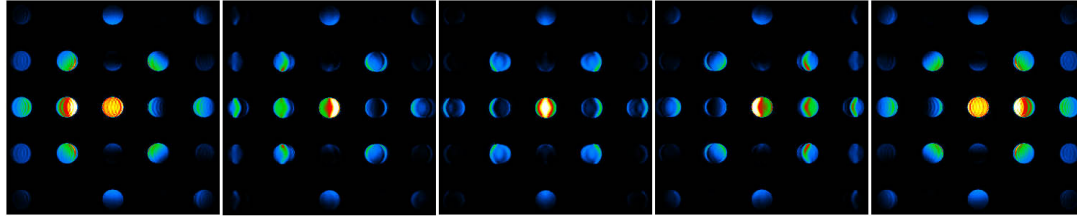


Figure S4: Diffraction patterns calculated from the supercell shown in Figure S3b), left to right these are: 8 nm to the left of the boundary (position 1); 2 nm to the left of the boundary (position 4); at the boundary (position 5); 2 nm to the right of the boundary (position 6); 8 nm to the right of the boundary (position 9).

## References

- [1] K. Tsuda, M. Tanaka, Refinement of crystal structural parameters using two-dimensional energy-filtered CBED patterns, *Acta Crystallogr A*, 55 (1999) 939-954.
- [2] I. MacLaren, L.Q. Wang, O. Morris, A.J. Craven, R.L. Stamps, B. Schaffer, Q.M. Ramasse, S. Miao, K. Kalantari, I. Sterianou, I.M. Reaney, Local stabilisation of polar order at charged antiphase boundaries in antiferroelectric  $(\text{Bi}_{0.85}\text{Nd}_{0.15})(\text{Ti}_{0.1}\text{Fe}_{0.9})\text{O}_3$ , *APL Materials*, 1 (2013) 021102.
- [3] K. Kalantari, I. Sterianou, S. Karimi, M.C. Ferrarelli, S. Miao, D.C. Sinclair, I.M. Reaney, Ti-Doping to Reduce Conductivity in  $\text{Bi}_{0.85}\text{Nd}_{0.15}\text{FeO}_3$  Ceramics, *Adv. Func. Mater.*, 21 (2011) 3737-3743.
- [4] I.M. Reaney, I. MacLaren, L.Q. Wang, B. Schaffer, A. Craven, K. Kalantari, I. Sterianou, S. Karimi, D.C. Sinclair, Defect chemistry of Ti-doped antiferroelectric  $\text{Bi}_{0.85}\text{Nd}_{0.15}\text{FeO}_3$ , *Appl. Phys. Lett.*, 100 (2012) 182902.
- [5] I. MacLaren, L.Q. Wang, B. Schaffer, Q.M. Ramasse, A.J. Craven, S.M. Selbach, N.A. Spaldin, S. Miao, K. Kalantari, I.M. Reaney, Novel Nanorod Precipitate Formation in Neodymium and Titanium Codoped Bismuth Ferrite, *Adv. Func. Mater.*, 23 (2013) 683-689.